Intrinsic Lipid Preferences and Kinetic Mechanism of *Escherichia coli* MurG[†]

Lan Chen, Hongbin Men, Sha Ha, Xiang-Yang Ye, Livia Brunner, Yanan Hu, and Suzanne Walker*

Department of Chemistry, Princeton University, Princeton, New Jersey 08544

Received February 12, 2002; Revised Manuscript Received March 26, 2002

ABSTRACT: MurG, the last enzyme involved in the intracellular phase of peptidoglycan synthesis, is a membrane-associated glycosyltransferase that couples *N*-acetyl glucosamine to the C4 hydroxyl of a lipid-linked *N*-acetyl muramic acid derivative (lipid I) to form the β-linked disaccharide (lipid II) that is the minimal subunit of peptidoglycan. Lipid I is anchored to the bacterial membrane by a 55 carbon undecaprenyl chain. Because this long lipid chain impedes kinetic analysis of MurG, we have been investigating alternative substrates containing shortened lipid chains. We now describe the intrinsic lipid preferences of MurG and show that the optimal substrate for MurG in the absence of membranes is not the natural substrate. Thus, while the undecaprenyl carrier lipid may be critical for certain steps in the biosynthetic pathway to peptidoglycan, it is not required—in fact, is not preferred—by MurG. Using synthetic substrate analogues and products containing different length lipid chains, as well as a synthetic dead-end acceptor analogue, we have also shown that MurG follows a compulsory ordered Bi Bi mechanism in which the donor sugar binds first. This information should facilitate obtaining crystals of MurG with substrates bound, an important goal because MurG belongs to a major superfamily of NDP−glycosyltransferases for which no structures containing intact substrates have yet been solved.

The increasing frequency of resistance to existing antibiotics is a serious problem (*1*). Structural and mechanistic information on essential bacterial enzymes could lead to the development of antibiotics that are active against resistant microorganisms. Both Gram-positive and Gram-negative bacterial cells are surrounded by layers of peptidoglycan, a cross-linked carbohydrate polymer that protects the cells from rupturing under high internal osmotic pressures. Many of the best antibiotics function by inhibiting peptidoglycan synthesis, and intense effort has been focused recently on the enzymes that synthesize peptidoglycan because all of them are potential targets for the design of new antibiotics.

MurG, the last enzyme in the intracellular phase of peptidoglycan synthesis (*2*), is a glycosyltransferase that catalyzes the transfer of *N*-acetyl glucosamine (NAG)[1] from UDP to the C4 hydroxyl of an *N*-acetyl muramic acid (NAM) derivative, lipid I, which is anchored to the cytoplasmic surface of the bacterial membrane. The product of the MurG reaction is a β-linked disaccharide commonly known as lipid II (Scheme 1). Once formed, this disaccharide is translocated across the bacterial membrane where it is polymerized and cross-linked to form the peptidoglycan layers. MurG has been shown to be essential for bacterial cell survival (*3, 4*), making this enzyme interesting to evaluate as a potential antibiotic target.

MurG activity was first described in the 1960s (*5*), but the protein was not purified until the latter half of the 1990s because of complications in monitoring the enzymatic activity (*6*−*8*). MurG proved challenging to study because its acceptor substrate, lipid I (compound **1** in Figure 1), is present in tiny quantities in bacterial cells and contains a 55-carbon lipid chain that makes it extremely difficult to handle. Because lipid I is so hard to obtain from natural sources and to manipulate, initial studies on MurG were carried out using crude cell membrane preparations containing lipid I generated in situ (*9*−*11*). This approach to studying MurG did not permit detailed analysis of the purified enzyme.

Van Heijenoort and co-workers reported in 1993 that *Escherichia coli* MurG is located on the cytoplasmic surface of the bacterial membrane (*12*), but sequence analysis suggested that there were no transmembrane spanning regions (*12*−*14*). Speculating that it would be possible to purify the enzyme and monitor its activity using soluble substrates in a membrane-free environment, we synthesized a lipid I analogue containing a 10 carbon citronellyl chain (**2**) in place of the natural undecaprenyl chain (*6*, *7*, *15*, *16*). MurG recognized the soluble lipid I analogue **2**, forming the basis for a direct activity assay. MurG proved to be straightforward to overexpress, purify, and maintain in soluble form at high concentrations in aqueous buffer. Following preliminary characterization of MurG using analogue **2** (*7*), we were able to crystallize this enzyme and solve the X-ray structure (*17*).

[†] This work was supported by NIH Grant R01-AI44854.

* To whom correspondence should be addressed. Phone: (609) 258-1149. Fax: (609) 258-2617. E-mail: swalker@princeton.edu.

[1] Abbreviations: UDP, uridine 5′-diphosphate; *E. coli*, *Escherichia coli*; BGT, T4 β-glucosyl transferase; CAZY, carbohydrate-active enzymes; NDP, nucleotide diphosphate; HEPES, 4-(2-hydroxyethyl)-1-piperazineethanesulfonic acid; NADH, reduced nicotinamide adenine dinucleotide; UDP−GlcNAc, uridine 5′-diphospho-*N*-acetylglucosamine; DMSO, dimethyl sulfoxide; THF, tetrahydrofuran; *m*-CPBA, *m*-chloroperoxybenzoic acid; DMF, *N*,*N*-dimethylformamide; TMSE, 2-(trimethylsilyl)ethyl; TEOC, 2-(trimethylsilyl)ethoxyl carbonyl; EDTA, *N*,*N*′-(1,2-ethanediyl)bis[(*N*-carboxymethyl)glycine]; PEP, phospho-(enol)pyruvate; GTB, human blood group B glycosyltransferase; NAG, *N*-acetylglucosamine; NAM, *N*-acetylmuramic acid; PBP, penicillin-binding protein; TDP, thymidine 5′-diphosphate; GtfB, vancomycin aglycone glycosyltransferase; FAB-MS: fast atom bombardment mass spectrometry; ESI-MS, electron spray ionization mass spectrometry.

10.1021/bi0256678 CCC: $22.00
Published on Web 05/02/2002

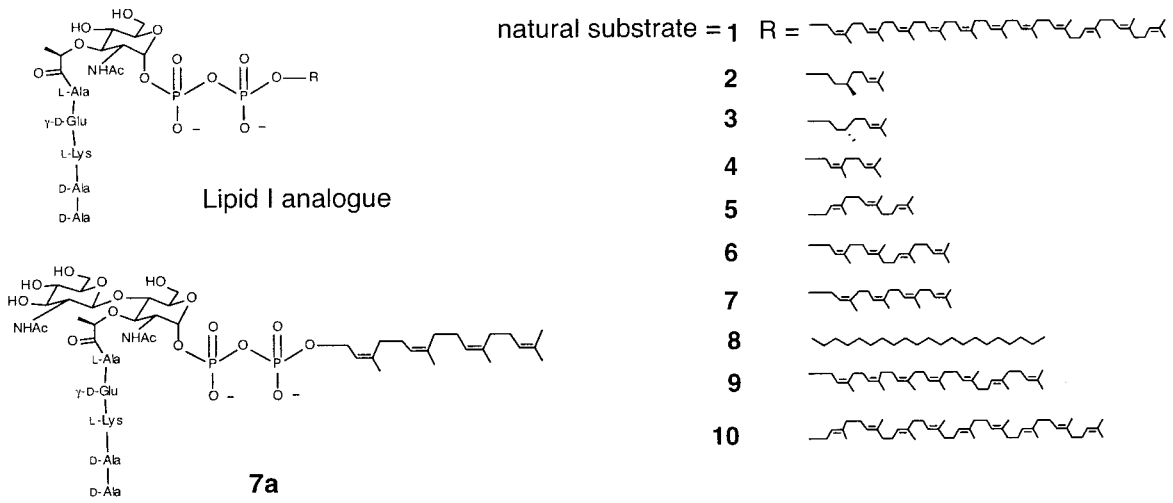

FIGURE 1: Structures of lipid I analogues and lipid II analogue **7a**.

Scheme 1

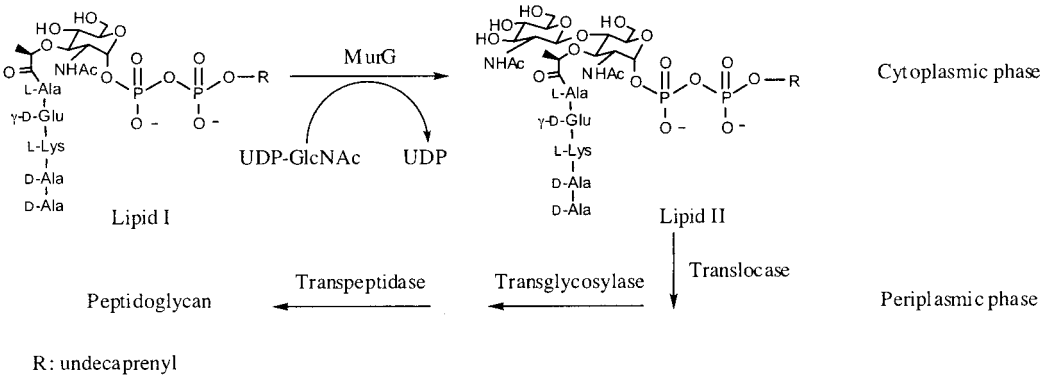

The X-ray structure of MurG revealed that this enzyme belongs to a superfamily of glycosyltransferases that includes phage T4 β-glucosyl transferase (BGT) (*18*, *19*), as well as members of CAZy (*20*) families 1 (*21*), other members of family 28, and probably also families 3, 4, and 5 (*22*−*25*). Detailed information on how donor sugars bind to the BGT/MurG superfamily would shed more light on the catalytic mechanism and on the molecular basis for hexose selectivity. Structural information could also facilitate the design of inhibitors to this class of enzymes. Unfortunately, neither we nor others have been able to obtain a co-complex of any member of the family with an intact UDP−sugar donor bound (*17*, *19*, *21*).

Some sequential enzymes that couple two substrates bind the substrates in a particular order (*26*). For these enzymes, it is not possible to crystallize a Michaelis complex with the substrate that binds second unless the first substrate is also present. It has been suggested that glycosyltransferases related to MurG might utilize an ordered mechanism in which the acceptor binds first, which would make it impossible to crystallize them with the donor sugar alone (*21*). The kinetic mechanism of only one enzyme belonging to the BGT/MurG superfamily has been previously investigated. This enzyme, OleD (CAZy family 1), glycosylates the macrolide oleandomycin and was shown to proceed through an ordered mechanism in which the donor sugar binds only after the macrolide is bound (*27*). We undertook experiments to determine the kinetic mechanism of MurG because we wanted to know whether MurG proceeds through the same mechanism as OleD or whether other mechanisms are possible for enzymes in this superfamily. We also wanted to know the reaction order to facilitate efforts to obtain crystalline co-complexes of MurG with substrates bound. As we began to probe the kinetic mechanism of MurG, it became apparent that a better substrate was needed to monitor the reaction than the one used in previous work (*6*, *7*). To find a better substrate, it was necessary to address an issue that we had deferred earlier, namely, the role of the lipid chain on the *N*-acetyl muramic acid pyrophosphoryl acceptor. Accordingly, we synthesized, for the first time, natural lipid I (*28*, *29*) as well as a set of lipid I analogues in which both lipid lengths and double-bond geometries were varied (Figure 1).

Herein, we describe the preferences of MurG with regard to lipid structure. We have identified a substrate that is substantially better than both the natural undecaprenyl-linked substrate and the citronellyl-linked substrate used in our earlier studies. Using a combination of synthetic substrate and product analogues, as well as a dead-end acceptor analogue, we were able to address the mechanism of MurG. Like OleD, it utilizes a sequential ordered Bi Bi mechanism; however, in the case of MurG, the donor sugar binds before the acceptor. Therefore, this superfamily of enzymes can utilize different kinetic mechanisms. The results reported here have implications for the design of experiments to obtain co-complexes of MurG with substrates bound. Because it has been speculated that the MurG family of glycosyltransferases is modular (*21*, *30*), these results may also have

implications for the design of reengineered glycosyltransferases in which donor and acceptor domains from different enzymes are recombined to achieve new selectivities.

MATERIALS AND METHODS

Materials. E. coli MurG was expressed and purified to homogeneity as described (*7*). Pyruvate kinase (type III from rabbit muscle, lyophilized powder, salt free), L-lactic dehydrogenase (type XXXIX from rabbit muscle, solution in 50% glycerol, potassium phosphate buffer, pH = 7.5), Tris (HCl), HEPES, phospho(enol)pyruvate (monopotassium salt), NADH, UDP, and UDP−GlcNAc were purchased from Sigma. Triton X-100 was purchased from Fluka.

Synthesis. The synthesis of lipid I analogues (**1**−**10**), as well as lipid II analogue **7a**, was carried out as previously described (*6*, *7*, *28*).

*Benzyl 2-Acetamido-6-O-acetyl-2-deoxy-3-O-[(R)-1-(methoxycarbonyl)ethyl]-α-D-glucopyranoside (**13**).* DMSO (2.54 mL, 35.9 mmol) was slowly added to a cold (−60 °C) stirred solution of oxalyl chloride (3.6 mL, 2.0 M, 7.2 mmol) in CH_2Cl_2 (7 mL). After the mixture was stirred at −60 °C for 20 min, a solution of the readily available protected saccharide **11** (*31*) (630 mg, 1.4 mmol) in 7 mL of CH_2Cl_2 was added, and the mixture was stirred at −60 °C for 1 h. Triethylamine (5 mL, 35.8 mmol) was slowly added, and then the mixture was allowed to warm to −30 °C in 30 min and kept at −30 °C for another 20 min. The reaction was quenched by adding aqueous $NaHCO_3$. The mixture was extracted with ethyl acetate three times. The organic layers were combined, washed with brine once, dried over sodium sulfate, filtered, and concentrated. The crude product **12** was used in the next step without further purification.

The ketone **12** was dissolved in 14 mL of anhydrous THF, and the solution was cooled to −78 °C. K-selectride (2.0 M, 1.72 mL, 1.72 mmol) was added, and the reaction was stirred at −78 °C for 30 min and quenched with acetone. Aqueous $NaHCO_3$ was added, and the mixture was extracted three times with EtOAc. The organic layers were combined and washed with brine once, dried over sodium sulfate, and concentrated. The residue was purified by flash chromatography (70% EtOAc/petroleum ether) to give 380 mg (60%, 2 steps) of product **13** as a white powder. R_f 0.42 (EtOAc). ^{1}H NMR ($CDCl_3$, 400 MHz) δ: 7.24−7.40 (m, 5H), 5.34 (d, J = 3.6 Hz, 1H), 4.58 (dd, J = 11.8, 61.0 Hz, 2H), 4.36 (q, J = 5.5 Hz, 1H), 4.26 (m, 2H), 4.20 (q, J = 7.0 Hz, 1H), 4.01 (m, 1H), 3.95 (t, J = 6.8 Hz, 1H), 3.78 (s, 3H), 3.68 (dd, J = 3.2, 11.2 Hz, 1H), 2.09 (s, 3H), 2.04 (s, 3H), 1.47 (d, J = 7.0 Hz, 3H). FAB-MS: calcd for $C_{21}H_{30}NO_9$ [M + H^+], 440; found, 440.

*Benzyl 2-Acetamido-6-O-acetyl-2,4-dideoxy-4-fluoro-α-muramic Acid Methyl Ester (**14**).* To a solution of **13** (460 mg, 1.05 mmol) in CH_2Cl_2 (10 mL) was added diethylamino sulfur trifluoride (0.2 mL, 1.57 mmol) at −50 °C. The solution was allowed to warm to room temperature and stirred for 1 h. Methanol was added to quench the reaction after it was cooled to −10 °C. The mixture was concentrated, and the residue was purified by flash chromatography (EtOAc) to give 370 mg (80%) of product as a white powder. R_f 0.59 (EtOAc). ^{1}H NMR ($CDCl_3$, 400 MHz) δ: 7.25−7.40 (m, 5H), 5.36 (d, J = 7.4 Hz, 1H), 4.60 (dd, J = 12.0, 47.0 Hz, 2H), 4.46 (q, J = 7.0 Hz, 1H), 4.16−4.30 (m, 3H), 3.90 (m, 1H), 3.84 (m, 2H), 3.78 (s, 3H), 2.12 (s, 3H), 2.04 (s, 3H), 1.48 (d, J = 7.0 Hz, 3H). ^{13}C NMR ($CDCl_3$, 100 MHz) δ: 175.6, 171.4, 171.0, 137.4, 128.7, 128.2, 128.1, 96.5, 91.6 (d, J = 182.0 Hz), 75.5 (d, J = 48.8 Hz), 70.7, 67.5 (d, J = 23.3 Hz), 62.2, 53.7, 53.6, 52.6, 23.2, 21.0, 19.1. ^{19}F NMR ($CDCl_3$, 376 MHz) δ: −25.84 (d, J = 54.7 Hz). FAB-MS: calcd for $C_{21}FH_{29}NO_8$ [M + H^+], 442; found, 442.

*Dibenzyloxyphosphonyloxy-2-acetamido-6-O-acetyl-2,4-dideoxy-4-fluoro-α-muramic Acid Methyl Ester (**15**).* To a solution of compound **14** (220 mg, 0.50 mmol) in 10 mL of MeOH was added 20 mg of 20% Pd−C. The reaction vessel was filled with hydrogen. After stirring at room temperature for 30 min, the suspension was filtered over Celite, and the catalyst was rinsed with methanol. The filtrate was concentrated to give a crude product, which was used in the next reaction without further purification.

The crude product from the previous step was premixed with 1*H*-tetrazole (70 mg, 1.0 mmol) and coevaporated with dry toluene and then dissolved in 10 mL of CH_2Cl_2. The reaction was cooled to −20 °C and dibenzyl *N*,*N*-diisopropylphosphoramidite (0.34 mL, 1.0 mmol) was added. The reaction was stirred at room temperature for 1 h and then cooled to −40 °C, and *m*-CPBA (610 mg, 70%, 2.5 mmol) was added. After stirring for 30 min at 0 °C and another 30 min at room temperature, the reaction was diluted with 50 mL of CH_2Cl_2 and washed with 10% aqueous Na_2SO_3 (2 × 50 mL), water (50 mL), and brine (50 mL). The CH_2Cl_2 layer was dried over anhydrous sodium sulfate, filtered, concentrated, and purified by flash chromatography (90% EtOAc/petroleum ether) to give 210 mg (70%) of **15** as a white solid. R_f 0.41 (90% EtOAc/petroleum ether). ^{1}H NMR ($CDCl_3$, 400 MHz) δ: 7.20−7.40 (m, 10H), 6.00 (br s, 1H), 4.98 (dd, J = 3.1, 11.0 Hz, 4H), 4.46 (t, J = 9.0 Hz, 1H), 4.35 (m, 2H), 4.10 (m, 2H), 3.95 (m, 1H), 3.75 (m, 1H), 3.69 (s, 3H), 1.89 (s, 3H), 1.78 (s, 3H), 1.36 (d, J = 6.6 Hz, 3H). ^{13}C NMR ($CDCl_3$, 100 MHz) δ: 175.3, 171.2, 170.4, 135.5, 135.4, 128.6, 127.9, 95.0, 90.4 (d, J = 182.7 Hz), 75.2, 74.6 (d, J = 17.1 Hz), 69.5, 69.0 (d, J = 24.0 Hz), 61.5, 53.2, 52.5, 22.7, 20.6, 18.7. ^{19}F NMR ($CDCl_3$, 376 MHz) δ: −26.65 (dd, J = 10.7, 50.8 Hz). FAB-MS: calcd for $C_{28}FH_{35}NO_{11}PNa$ [M + Na^+], 634; found, 634.

*2-Acetamido-1-α-dibenzyloxyphosphonyloxy 2,4-Dideoxy-4-fluoromuramic Acid (**16**).* To a solution of **15** (85 mg, 0.14 mmol) in MeOH/H_2O (1.8:0.6 mL) was added LiOH (16.5 mg, 0.4 mmol). The reaction was stirred at room temperature for 30 min and then diluted with 10 mL of MeOH. After neutralizing with AcOH, the solution was concentrated, and the residue was purified by flash chromatography (15% MeOH/$CHCl_3$, 0.1% AcOH) to give 74 mg (96%) of product **16** as a white powder. R_f 0.19 (10% MeOH/$CHCl_3$). ^{1}H NMR (CD_3OD, 500 MHz) δ: 7.40−7.30 (m, 10H), 6.09 (br s, 1H), 5.08 (dd, J = 5.9, 8.3 Hz, 4H), 4.56 (dt, J = 9.5, 50.9 Hz, 1H), 4.39 (q, J = 7.0 Hz, 1H), 3.82 (m, 1H), 3.72 (m, 2H), 3.64 (m, 2H), 1.87 (s, 3H), 1.43 (d, J = 7.0 Hz, 3H). ^{13}C NMR (CD_3OD, 125 MHz) δ: 179.3, 174.1, 137.14, 137.06, 129.9, 129.3, 96.8, 91.3 (d, J = 180.2 Hz), 77.5, 76.1 (d, J = 17.8 Hz), 73.5 (d, J = 24.2 Hz), 71.2, 60.8, 55.2, 22.7, 19.6. ^{19}F NMR (CD_3OD, 376 MHz) δ: −28.6 (dd, J = 12.7,

50.9 Hz). FAB-MS: calcd for $C_{25}FH_{31}NO_{10}PNa$ [M + Na^+], 578; found, 578.

*2-Acetamido-2,4-dideoxy-4-fluoro-1-α-muramyl Phosphate Pentapeptidyl Ester (**17**).* To a solution of compound **16** (74 mg, 0.13 mmol) and NH_2-L-Ala-γ-D-Glu(*O*-TMSE)-L-Lys-(*N*-TEOC)-D-Ala-D-Ala-*O*-TMSE (103 mg, 0.13 mmol) in 2.5 mL of DMF was added diisopropylethylamine (108 mL, 0.62 mmol) followed by HOBt (33.5 mg, 0.25 mmol) and pyBOP (129 mg, 0.25 mmol). After stirring at 0 °C for 30 min, the reaction was purified by flash chromatography (EtOAc; then 5% MeOH/EtOAc) to give 110 mg (65%) of the dibenzyl phosphate as a white solid. R_f 0.6 (10% MeOH/EtOAc). To a solution of this dibenzyl phosphate (110 mg, 0.08 mmol) in 5 mL of MeOH was added 10 mg of 20% Pd−C. The reaction vessel was filled with hydrogen and stirred at room temperature. A total of 0.1 mL of diisopropylethylamine was added after 30 min. The solution was diluted with 15 mL of MeOH and stirred for 30 min. The catalyst was filtered off over Celite. The filtrate was concentrated to give **17**. R_f 0.31 ($CHCl_3$/MeOH/H_2O = 3:2:0.5).

*P^1-2-Acetamido-2,4-dideoxy-4-fluoro-α-muramyl Pentapeptidyl Ester P^2-Nerylneryl Diphosphate (**19**).* Nerylneryl phosphate **18** (*32*−*34*) (30 mg, 0.074 mmol) was coevaporated with diisopropylethylamine and toluene three times and then dissolved in 1.6 mL of THF. To the solution was added 1,1′-carbonyldiimidazole (51.4 mg, 0.32 mmol). After 1.5 h, 32 μL of dry MeOH was added, and the reaction was stirred for 1 h. The solvent was evaporated to give the phosphoimidazole intermediate.

Monophosphate **17** (92 mg, 0.064 mmol) was coevaporated with diisopropylethylamine and toluene and then dissolved in DMSO/THF (0.8:0.8 mL) and transferred to the phosphoimidazole intermediate. The reaction was stirred at room temperature for 3 days. The volume was reduced under vacuum, and the residue was loaded to a C18 reverse phase column (8 mm × 80 mm, particle size 40 mm, pore size 60 Å, from J. T. Baker) and eluted with CH_3CN/10 mM NH_4HCO_3 aqueous solution (0, 5%, 10%, 15%, 20%, 25%, 30%, 40% of 10 mL each). The fractions containing desired product were combined and concentrated to give a crude product. Starting material **17** (60 mg) was recovered. R_f 0.62 ($CHCl_3$/MeOH/H_2O = 4:2:0.5).

To a 0.4 mL solution in DMF of the crude product from the previous step was added tetrabutylammonium fluoride (1.0 M in THF, 0.4 mL). The reaction was stirred at room temperature for 16 h. Solvent was removed under vacuum. The residue was loaded to a C18 reverse phase column (8 mm × 80 mm, particle size 40 μm, pore size 60 Å, from J. T. Baker) and eluted with CH_3CN/20 mM NH_4HCO_3 aqueous solution (0, 5%, 10%, 15%, 20%, 25%, 30% of 10 mL each). The purification procedure was repeated one more time to give 20 mg of **19** (74% based on the recovery of **17,** 2 steps) as an ammonium salt. R_f 0.20 ($CHCl_3$/MeOH/H_2O = 3:2:0.5). ^{1}H NMR (CD_3OD, 500 MHz) δ: 5.50 (m, 1H), 5.40 (m, 1H), 5.09 (m, 3H), 3.65−4.58 (m, 12H), 2.88 (m, 2H), 2.27 (m, 4H), 1.45−2.10 (m, 38H), 1.42 (d, *J* = 7.0 Hz, 3H), 1.34 (m, $3CH_3$). ^{19}F NMR (CD_3OD, 376 MHz) δ: −26.2 (dd, *J* = 53.7, 12.3 Hz). ESI-MS: calcd for $C_{51}FH_{85}O_{20}N_7P_2$ [M − H^-], 1196; found, 1196.

*Enzymatic Synthesis of Lipid II Analogue **7a**.* The lipid II analogue **7a** was prepared from the corresponding synthetic lipid I analogue **7** using purified MurG (*28*). A total of 3.35 mg of **7** was dissolved in 0.5 mL of MeOH and added to 8.89 mL of MurG reaction buffer (50 mM HEPES, pH 7.9, 5 mM $MgCl_2$) followed by 40 μL of 100 mM UDP−GlcNAc and 0.57 mL of 2.66 mg/mL MurG stock (in 20 mM Tris, pH = 7.9, 150 mM NaCl, and 50 mM EDTA). After 30 min, another 40 μL of 100 mM UDP−GlcNAc was added. The reaction was poured into 50 mL of ice-cold MeOH, and the solution was concentrated to ∼2 mL, and then the mixture was purified over a C18 column. The disaccharide product was eluted with 30−50% acetonitrile. The small amount of lipid I remaining in the product was converted to lipid II by repeating the reaction a second time. The final yield of pure lipid II analogue **7a** was quantitative.

Fluorometric Assay. Reactions were carried out in 96- or 384-well microplates, and the decrease in NADH fluorescence was monitored at 465 nm using a Perkin-Elmer HTS 700 Plus Bio-Assay plate reader. Each reaction contained MurG reaction buffer (50 mM HEPES, pH = 7.9, 5 mM $MgCl_2$, and, except where noted, 0.2% Triton X-100), 0.5 mM phospho(enol)pyruvate (PEP), 0.2 U/μL of lactic dehydrogenase, 3 U/μL of pyruvate kinase (added as 10 U/μL stock solution in 100 mM K_2HPO_4, pH = 7.6), 0.25 mM NADH, 15% methanol (except where noted otherwise), an appropriate amount of UDP−GlcNAc, lipid I analogue (added as an aliquot from a concentrated stock solution in water or methanol), and 0.5−10 μL of enzyme 100-fold diluted from a concentrated stock (in 20 mM Tris, pH = 7.9, 150 mM NaCl, and 50 mM EDTA). Reaction volumes were 100 μL for the 96-well plates and 30 μL for the 384-well plates. All of the components except for the MurG substrates and MurG were premixed in a reservoir and dispensed into each well. The substrates were then added, and the reaction mixtures were incubated for 5−10 min until a stable background rate was achieved (typically corresponding to 1 μM/min decrease in NADH). MurG was then added and the fluorescence was monitored for 15−20 min. A time course for each reaction was obtained. The initial rates were determined by calculating the slopes (linear fitting) of the initial linear portion of the reaction time course curves using KaleidaGraph (Synergy Software). Calibration was done using a series of UDP solutions with known concentrations. One micromolar UDP corresponds to 500 fluorescence units (RFU) under the instrument settings. We note that the K_m value reported here for **2** using the fluorescence assay is approximately 10-fold higher than that reported earlier using the biotin capture assay (*7*). Some of the increase may be due to changes in the specific reaction conditions—for example, the inclusion of detergent or additives that become inhibitory at high concentrations such as postassium ion. In addition, the fluorescent assay mixture contains relatively high concentrations of other enzymes that may bind substrates nonspecifically.

Measuring the Relative Activities of Lipid I Analogues. The initial reaction rates of the analogues were measured at acceptor concentrations of 100 μM. The analogues were added to the reaction mixture as methanol solutions. For these experiments, the reaction volumes were 100 μL, the UDP−GlcNAc concentration was 20 mM, and Triton X-100 was omitted from the MurG reaction buffer. Relative rates are ratios of the reaction rates reported in fluorescence units/min (RFU/min).

Scheme 2

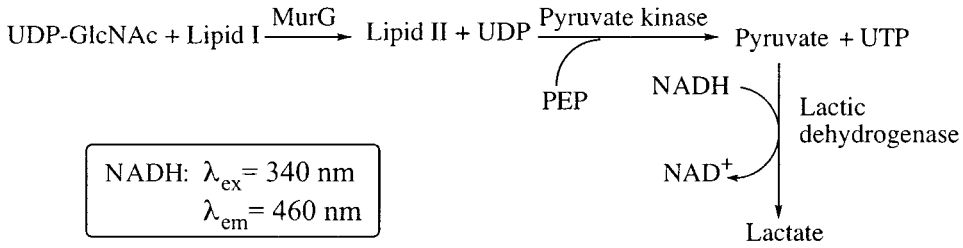

Obtaining Kinetic Parameters. Kinetic measurements were carried out by keeping one substrate at a constant concentration and varying the other. For the kinetic measurements of lipid I substrates, UDP−GlcNAc was fixed at a concentration of 2−10 mM (at least 10 times its K_m). For the measurements of UDP−GlcNAc, the lipid I concentration was fixed at 100 μM (about twice its K_m) because of the limited supply of the synthetic substrate. K_m and k_{cat} values were determined by fitting the initial rates to the Michaelis−Menten equation using KaleidaGraph. IC_{50} measurements were done by keeping both substrates at their K_m values and fitting initial rates to the equation $v_i/v_0 = 1/(1 + I/IC_{50})$, where v_0 is the initial rate in the absence of the inhibitor and v_i is the initial rate in the presence of the inhibitor. I is the concentration of the inhibitor.

Determining Inhibition Patterns. Inhibition studies were carried out at three to four different concentrations of the inhibitors. While determining the inhibition pattern with respect to UDP−GlcNAc, the concentration of the lipid I substrate was held at nonsaturating levels. For inhibition patterns with respect to lipid I, measurements were done with UDP−GlcNAc at both saturating and nonsaturating levels. The biotin capture assay described previously (*6*, *7*) was employed when UDP was used as an inhibitor. All of the other measurements were done using the continuous fluorometric assay described here.

K_{is} and K_{ii} were calculated from the replots of the double reciprocal curves using the following equations:

For competitive inhibition

$$\frac{1}{v} = \frac{1}{V} + \frac{K_m}{V}\left(1 + \frac{I}{K_{is}}\right)\frac{1}{S}$$

For uncompetitive inhibition

$$\frac{1}{v} = \frac{1}{V}\left(1 + \frac{I}{K_{ii}}\right) + \frac{K_m}{V}\frac{1}{S}$$

For noncompetitive inhibition

$$\frac{1}{v} = \frac{1}{V}\left(1 + \frac{I}{K_{ii}}\right) + \frac{K_m}{V}\left(1 + \frac{I}{K_{is}}\right)\frac{1}{S}$$

The K_i value for the fluoro sugar analogue **19** was determined by comparing the slopes of the double reciprocal plots in the presence of inhibitor to the one obtained in the absence of the inhibitor, using the following rate equation (*36*):

$$\frac{1}{v} = \frac{1}{V} + \frac{K_a}{VA} + \frac{K_b}{VB}\left(1 + \frac{I}{K_i}\right) + \frac{K_{ia}K_b}{VAB}$$

K_a and K_b are Michaelis−Menten constants of UDP−GlcNAc and the acceptor analogue **7**, respectively; K_{ia} is the dissociation constant of the MurG·UDP−GlcNAc complex, and V is the maximum rate.

Table 1: Reaction Rates (RFU/min) and Relative Reaction Rates of Lipid I Analogues[a]

LPI analogues	in 5% MeOH	in 15% MeOH	relative rate
1	undetectable	212	0.014
2	499	1043	0.068
3	ND[b]	518	0.034
4	ND[b]	4433	0.29
5	1244	1588	0.11
6	3321	10 335	0.68
7	ND[b]	15 182	1
8	1952	3957	0.26
9	1026	2059	0.14
10	undetectable	232	0.015

[a] The initial reaction rates (RFU/min after subtracting the background rate) of the analogues were measured under identical conditions at acceptor concentrations of 100 μM and a UDP−GlcNAc concentration of 20 mM. Relative rates are ratios of the reaction rates reported in fluorescence units/min. [b] Not determined.

RESULTS

Evaluation of Acceptor Analogues. Following routes developed previously in our laboratory (*6*, *7*), we prepared natural lipid I (*28*) and a set of lipid I analogues containing lipid chains with varying lengths and double-bond geometries. The set of compounds, shown in Figure 1, includes the enantiomer (**3**) of the citronellyl analogue (**2**) used in our initial studies of MurG.

To evaluate the compounds, we adapted a fluorescence assay that was first used to monitor glycosyltransferase activity by Palcic and co-workers (*35*). In this assay, the formation of the UDP product is detected by coupling its formation to the NADH-mediated reduction of pyruvate to lactate by lactic dehydrogenase, as shown in Scheme 2. The pyruvate is produced from phospho(enol)pyruvate, which phosphorylates UDP in the presence of pyruvate kinase. As the concentration of NADH decreases, the fluorescent signal at the emission wavelength of NADH decreases, and this decrease is monitored to obtain the reaction rate. Under the reaction conditions described, the reaction rate is linearly related to the MurG concentration at all relevant lipid I and UDP−GlcNAc concentrations.

The initial reaction rates of the acceptor analogues, measured under identical conditions, are reported in Table 1 (as RFU/min) along with the relative reaction rates. The data are summarized in the histograms in Figure 2. Although MurG converts all of these lipid I analogues to the corresponding lipid II analogues, it nevertheless displays clear preferences with respect to both chain length and double-bond geometry. MurG prefers lipids having a *cis*-allylic

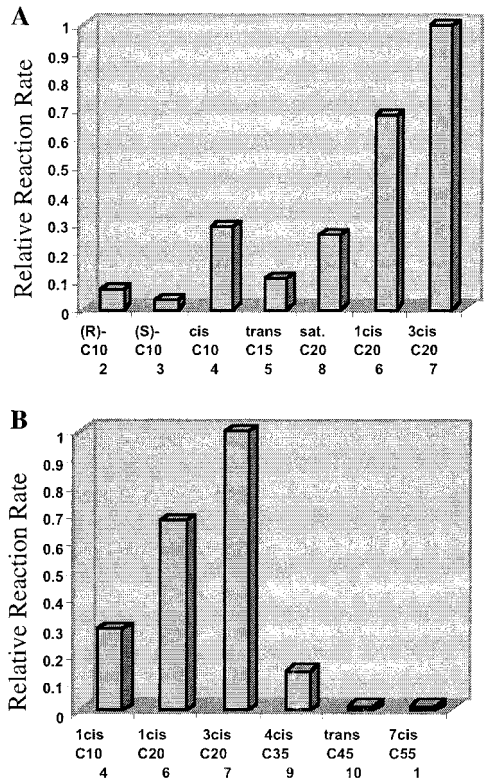

FIGURE 2: Histograms summarizing the relative reaction rates of lipid I analogues. (A) Dependence on lipid structure for analogues up to 20 carbons. (B) Dependence on lipid length for compounds containing *cis*-allylic double bonds (except **10**, which contains a *trans*-allylic double bond). The number of successive *cis*-isoprene units in each lipid is indicated.

double bond to other lipids. For example, the 10 carbon neryl derivative **4** reacts significantly faster than the 10 carbon citronellyl derivatives **2** and **3** or than the 15 carbon all-trans farnesyl derivative **5**. Among the derivatives containing 20 carbon chains, the two having a *cis*-allylic double bond (**6** and **7**) react faster than the one having a simple alkane chain (**8**). There is also an optimum length requirement. Among the compounds containing cis double bonds allylic to the pyrophosphate linkage, the relative reaction rate increases with chain length up to four isoprene units and then decreases dramatically. The 35 carbon prenyl chain (**9**) is considerably worse than the 20 carbon chains (**6** and **7**); natural lipid I (**1**), which contains a 55 carbon chain, does not react detectably unless 15% methanol is added to the reaction. The low reactivity of natural lipid I and other long chain analogues is apparently due to their propensity to aggregate. Consistent with this hypothesis, the relative reaction rate of the natural lipid I was found to increase by a factor of 10 when 0.2% Triton X-100 was included in the buffer. Nevertheless, under the same conditions, compound **7** is still the best substrate of the series. On the basis of these studies, compound **7** was selected as the optimum substrate with which to monitor MurG activity in solution. Like the natural substrate, **7** has a cis double bond in the key allylic position as well as the following two isoprene units. However, **7** is considerably more soluble in water than natural lipid I. This compound was examined in more detail to obtain kinetic parameters.

*The Catalytic Efficiency of the Optimal Substrate Analogue **7***. The kinetic parameters of compound **7** were compared to those of the original substrate analogue **2** as described (Materials and Methods), and the catalytic efficiency was found to be 65 times higher. At saturating UDP−GlcNAc concentrations, K_m(**7**) = 0.053 ± 0.006 mM, k_{cat} = 837 min^{-1} and k_{cat}/K_m(**7**) = 15 791 mM^{-1} min^{-1}, whereas K_m(**2**) = 0.553 ± 0.125 mM, k_{cat} = 134 min^{-1}, and k_{cat}/K_m(**2**) = 241 mM^{-1} min^{-1}. Much of the increase in efficiency is due to a decrease in the Michaelis constant for **7** compared to that for **2**. We conclude, therefore, that the lipid chain interacts with the enzyme. Because the preferred substrate is identical to the natural substrate over the first few isoprene units, MurG apparently recognizes the first part of the undecaprenyl chain.

The increased catalytic efficiency of the optimal substrate means that we can now easily carry out kinetic analyses of MurG point mutants with compromised activity to probe the role of selected amino acid side chains in catalysis. Furthermore, as demonstrated below, it is possible to use a combination of acceptor/product pairs with differential affinities for the enzyme to probe the mechanism.

Product Inhibition Analysis. Our initial failures to obtain co-complexes of MurG with either UDP−GlcNAc or lipid I analogues prompted us to explore the mechanism of the enzyme. Like other inverting NDP−glycosyltransferases that have been investigated (*27*, *37*−*40*), MurG utilizes a sequential reaction mechanism in which both substrates bind to the enzyme to form a ternary complex prior to reaction. To design crystallization trials to obtain co-complexes of sequential enzymes, it is useful to know whether the substrates bind in a compulsory order and, if so, to know which substrate binds first. Because the rate equations describing an enzymatic reaction change in the presence of inhibitors, inhibition patterns can permit one to determine the kinetic mechanism (*36*, *41*). Product inhibition experiments are often the simplest means of probing mechanism (*26*) because the products of an enzymatic reaction can usually be readily obtained. Although these types of experiments are not always conclusive, they usually permit one to narrow down the possibilities. As described below, we used product inhibition analysis to narrow down the possible mechanisms and then synthesized a single dead-end substrate inhibitor to test the most likely mechanism.

The UDP product was found to be a competitive inhibitor of the UDP−GlcNAc donor and a noncompetitive inhibitor of the lipid I acceptor analogue (Table 2). This inhibition behavior ruled out an ordered Bi Bi mechanism in which the acceptor substrate binds first, but left open several other possibilities (*26*). Therefore, we evaluated a lipid II analogue as a product inhibitor to narrow the possibilities further.

Preliminary experiments showed that the IC_{50} value of lipid II analogue **7a** was higher than 1 mM when **7** was used as the acceptor substrate (data not shown). Using the **7**/**7a** acceptor/product pair, we estimated that it would take more than 10 mg of **7a** to complete a product inhibition analysis. However, acceptors with different lipid chains have different affinities for the enzyme (as inferred from the relative K_m values of **2** and **7**). Therefore, we took advantage of the fact that we had made a range of unnatural lipid I/II analogues to identify an acceptor/product pair that was more suitable for product inhibition analysis. Preliminary experiments showed that when **2** was used as the acceptor substrate, the IC_{50} of **7a** was only 48 μM, suggesting an inhibition constant

Table 2: Summary of Product Inhibition Patterns Obtained for MurG

inhibitor	varied substrate	fixed substrate	pattern	K_{is} (μM)	K_{ii} (μM)
UDP	UDP−GlcNAc	lipid I (unsatur)	C[b]	31.4 ± 3.76	
UDP	lipid I analogue **2b**[a]	UDP−GlcNAc (unsatur)	NC[c]	83.1 ± 14.88	23.1 ± 3.69
lipid II analogue **7a**	UDP−GlcNAc	lipid I (unsatur)	NC[c]	58.9 ± 24.51	52.2 ± 27.92
lipid II analogue **7a**	lipid I analogue **2**	UDP−GlcNAc (unsatur)	NC[c]	35.7 ± 9.98	30.3 ± 6.84
lipid II analogue **7a**	lipid I analogue **2**	UDP−GlcNAc (satur)	NC[c]	47.1 ± 6.75	131.5 ± 12.61

[a] **2b** is **2** derivatized on the lysine ϵ amino group with *N*-(+)-biotinyl-6-aminocaproyl (see refs *6*, *7*). [b] Competitive. [c] Noncompetitve.

Scheme 3

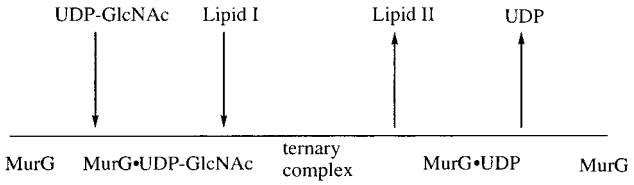

within a useful range for analysis.

Inhibition experiments at different concentrations of **7a** were carried out at varying acceptor **2** concentrations using both nonsaturating and saturating concentrations of the UDP−GlcNAc donor, and the product was found to be noncompetitive with respect to the acceptor. Product **7a** also proved to be a noncompetitive inhibitor of UDP−GlcNAc at nonsaturating concentrations of the acceptor. Combined with the results obtained using UDP as the product, these inhibition patterns (Table 2) are consistent with two mechanisms: an ordered Bi Bi mechanism in which the UDP−GlcNAc donor binds first, as shown in Scheme 3, or an iso-Theorell−Chance mechanism in which the acceptor binds first (*26*).

Only one glycosyltransferase that has been studied, human blood group B glycosyltransferase (GTB), has been proposed to utilize a Theorell−Chance mechanism (*42*). GTB is a retaining glycosyltransferase and is believed to operate via a double-displacement mechanism wherein a glycosyl-enzyme intermediate forms prior to the reaction with the second substrate, consistent with the Theorell−Chance mechanism. It seemed to us unlikely that the reaction of an inverting glycosyltransferase such as MurG would be compatible with a mechanism in which the presence of the ternary complex is kinetically insignificant. Nevertheless, we prepared a dead-end inhibitor of the acceptor substrate to distinguish between these two possible mechanisms and also to verify the mechanistic conclusions drawn from the product inhibition analysis. Verification was deemed necessary because the inhibition studies were predicated on the assumption that **7a** can actually be used as a product inhibitor of **2**, which contains a shorter lipid chain. Although this assumption is reasonable, **7a** is not the product of **2**. Furthermore, the noncompetitive patterns that dominate the product inhibition analysis in an ordered Bi Bi mechanism are not as reliable as other types of inhibition patterns for deducing mechanism. Hence, we prepared a dead-end substrate that would give a distinctive inhibition pattern if the proposed ordered Bi Bi mechanism were correct.

Dead-End Inhibition Analysis. A dead-end competitive inhibitor of a substrate that binds second in an ordered Bi Bi mechanism is expected to give a distinctive *uncompetitive* inhibition pattern with respect to the substrate proposed to bind first. Therefore, the 4-deoxy, 4-fluoro analogue (**19**) of the acceptor substrate **7** was prepared in 11 steps from the readily available protected *N*-acetyl muramic acid derivative **11** (*31*), as shown in Scheme 4. When the acceptor substrate **7** was varied, the double-reciprocal plots at different concentrations of **19** converged on the $1/v$ axis, indicating a competitive inhibition pattern, as expected on the basis of the structural resemblance between **7** and **19**. The K_i value for **19** was calculated to be 19.5 ± 1.6 μM.

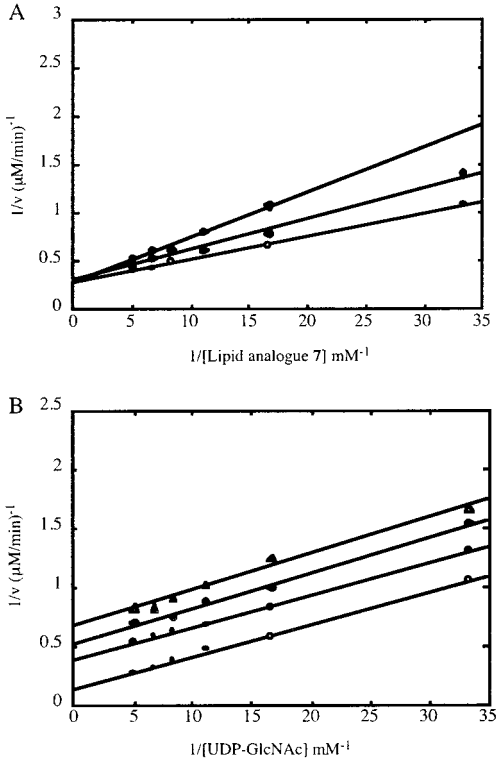

FIGURE 3: Lineweaver−Burke plots showing inhibition patterns with dead-end inhibitor **19**. (A) [UDP−GlcNAc] = 60 μM; [**19**] = 0 μM (○), 10 μM (◆), and 30 μM (◇). (B) [acceptor analogue **7**] = 60 μM; [**19**] = 0 μM (○), 10 μM (●), 20 μM (◇), and 30 μM (△).

With a suitable dead-end competitive inhibitor of **7** in hand, we were able to complete the mechanistic analysis. As shown in Figure 3, the double-reciprocal plots at different concentrations of **19** were found to be parallel when UDP−GlcNAc was the varied substrate, consistent with uncompetitive inhibition. The results confirm that MurG utilizes an ordered Bi Bi mechanism in which the donor binds first (*43*).

DISCUSSION

In this paper, we address two issues pertinent to understanding MurG. Both issues may have some relevance to other enzymes as well. One issue relates to the role of lipid structure on substrate recognition by MurG. MurG is

Scheme 4

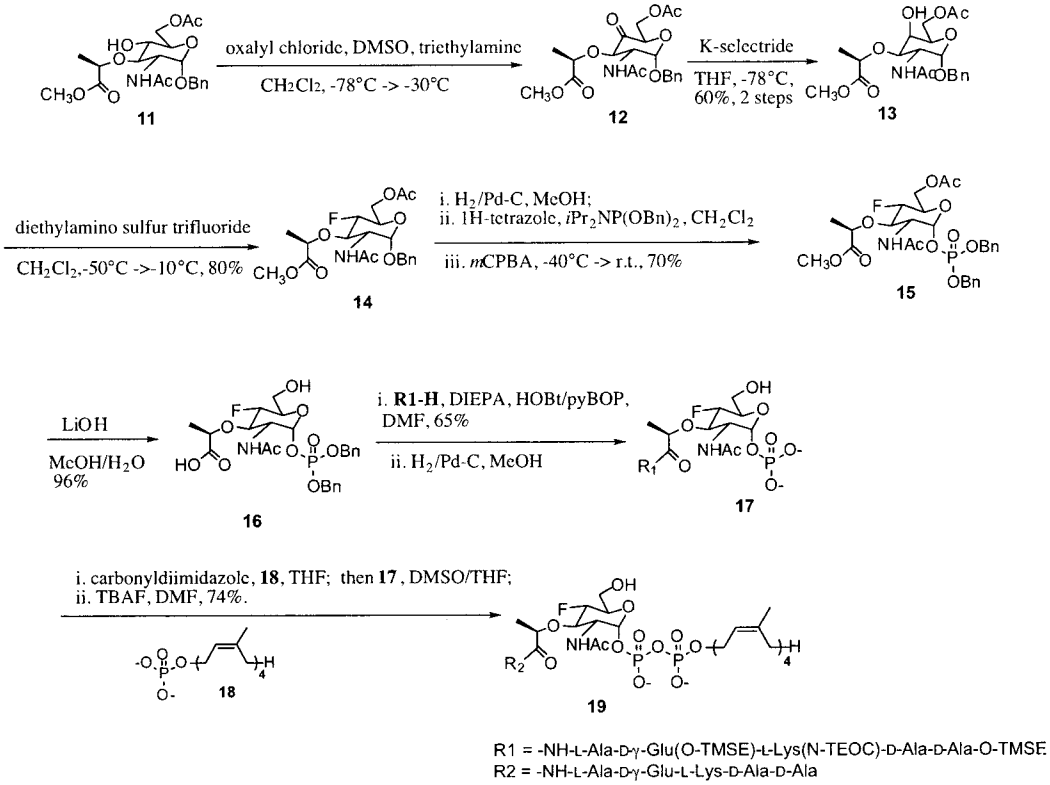

Scheme 5

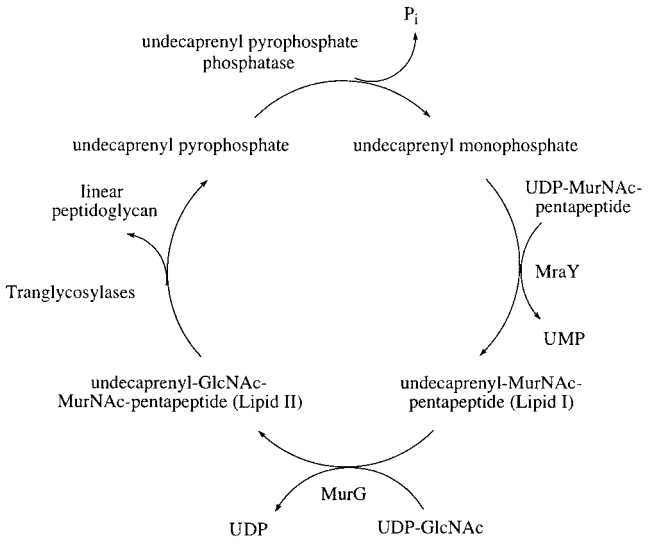

membrane-associated and converts a lipid-linked monosaccharide to a lipid-linked disaccharide. The lipid anchor on the monosaccharide substrate is a polyprenyl chain containing 11 isoprene units (55 carbons). The first seven isoprene units have cis double bonds. The rest have trans double bonds. As illustrated in Scheme 5, several enzymes in the biosynthetic pathway to peptidoglycan utilize substrates containing this undecaprenyl chain, but its exact function is unknown (*2*, *44*). Whether any of the enzymes in Scheme 5 absolutely require the undecaprenyl chain is also unknown. Information on the substrate lipid requirements for each of the enzymes involved in peptidoglycan synthesis could be useful for helping to understand the role of the undecaprenyl chain in the overall cycle. In addition, mechanistic studies on various enzymes would be facilitated by the use of substrates containing shorter lipid chains because the natural 55 carbon chain makes the compounds exceedingly difficult to handle.

We have shown here that MurG prefers substrates that contain lipid chains that are considerably shorter than that of the natural substrate. However, among the various shorter chain acceptor analogues, there are large differences in reaction rates. For example, compounds that contain a *cis*-allylic double bond react faster than compounds that do not. Because the natural substrate contains a *cis*-allylic double bond, this finding suggests that MurG recognizes the first part of the undecaprenyl lipid carrier. Consistent with this proposal, the best substrate (**7**) mimics the natural substrate over the first three isoprene units.

In previous work (*28*), we have investigated the substrate requirements of PBP1b, the major transglycosylase in *E. coli*, which is responsible for polymerizing lipid II. PBP1b has more stringent substrate requirements than MurG. For example, functional substrates for PBP1b must have a *cis*-allylic double bond and be significantly *longer* than 20 carbons. Nevertheless, in an in vitro assay, PBP1b still prefers an unnatural substrate with a shorter lipid to the natural undecaprenyl lipid II. Thus, while the undecaprenyl carrier lipid *may* play an essential role in certain steps of the peptidoglycan synthesis pathway—for example, translocation from the inner to the outer surface of the bacterial membrane (*44*)—several of the enzymes in the pathway require substrates containing only a portion of this lipid. Kinetic analysis of these enzymes under in vitro conditions is often greatly facilitated by the use of unnatural lipids.

Unnatural substrates may also simplify the study of other enzymes that function in metabolic pathways in which substrates are shuttled by a carrier lipid. Many such pathways exist in bacteria and fungi (*44*−*46*), and some have also been identified in higher eukaryotes (*47*, *48*). The lipid require-

ments of enzymes in most lipid-linked pathways have not been investigated extensively (*47*, *49*, *50*), but it seems likely that the full-length lipids play specialized roles (*44*, *51*). If so, it should be possible to prepare substrates with "better" physical properties for most of the other enzymes by mimicking the first part of the natural substrate and then varying the length.

It is worth commenting on the different length requirements for substrates of MurG and the bacterial transglycosylases because the differences may reflect fundamental differences in how these enzymes operate. It is likely that the transglycosylases are true interfacial enzymes (*52*). They contain membrane anchors that prevent them from dissociating readily from membranes (*53*). Furthermore, their substrates are embedded in the membrane, and turnover is speculated to be processive (*54*). The long lipid chain length preferences of the transglycosylases suggest that they require a membrane-like surface in which the substrates are in enforced proximity. MurG, on the other hand, is not an interfacial enzyme in the conventional sense (even though it functions at an interface) because it recruits one of its substrates from the cytoplasm. MurG accepts substrates with chains at least as short as 10 carbons, and these 10 carbon substrates, including the active neryl derivative (**4**), do not aggregate significantly in water even at millimolar concentrations. We have concluded that MurG does not need a membrane-like surface to function. To better understand the different lipid length preferences of MurG and transglycosylases, it will be necessary to characterize the aggregation states of all of the substrates; where aggregates exist at the concentrations used to study the enzymes. Kinetic models that take the interface into account (*52*) must be evaluated. Given the information we now have, however, we predict that transferases that operate on membrane-anchored substrates will show different lipid length requirements depending on whether both of their substrates are membrane-bound (which would suggest that the enzymes are truly interfacial) or only one is. If this prediction is borne out, it should be possible to make a reasonable guess a priori about how long the lipid chain of any given synthetic substrate of a membrane-bound enzyme would have to be for activity. Interfacial enzymes would be expected to prefer substrates that form micelles at the concentrations that were used.

The second issue that we address in this paper relates to the kinetic mechanism of MurG. MurG is a member of a major superfamily of glycosyltransferases that utilize UDP or TDP glycosyl donors or both. In addition to the MurG structure, there are two other crystal structures of enzymes belonging to this superfamily (*18*, *19*, *21*). One, BGT, is of a phage enzyme that glycosylates hydroxymethylcytosines on duplex DNA; the other, GtfB, is an enzyme that glycosylates aglycones of the vancomycin antibiotic group. None of the three structures has yet been crystallized with either acceptor or intact donor bound, and it would be enlightening to have co-complexes of enzymes belonging to this superfamily. In the short term, complexes with glycosyl donors would be of particular interest because the superfamily is largely defined by structural and sequence similarities in the C-terminal domain, which is the proposed donor binding domain (*7*, *17*, *22*−*25*). Structures with intact donors bound could shed light on the catalytic mechanism and might also provide insight into how the hexose selectivity is determined. Understanding the atomic basis for selectivity is a key step in learning how to alter selectivity.

Despite considerable effort, it has not yet been possible to obtain co-complexes of enzymes in this superfamily with intact donor. In the case of BGT, co-complexes with the UDP product rather than the UDP−sugar substrate have been obtained whenever efforts were made to crystallize the protein with the donor sugar (*18*, *19*). It was suggested that the donor sugar hydrolyzes too rapidly for an intact co-complex to be obtained. For GtfB, which has only been crystallized in the free enzyme form, it was suggested that the enzymatic mechanism might preclude obtaining a binary complex with the intact glycosyl donor (*21*). This suggestion was made on the basis of the only previously reported kinetic analysis of an enzyme belonging to the BGT/MurG/GtfB NDP−glycosyltransferase superfamily (*27*). The enzyme studied was OleD, a glycosyltransferase that glycosylates oleandomycin and that belongs, like GtfB, to CAZy family 1. OleD was shown to utilize an ordered mechanism in which the acceptor substrate binds first (*27*). If other enzymes in the same superfamily also proceed through this mechanism, one would not expect the intact donor to form a binary Michaelis complex with the enzyme. In this paper, we have shown that MurG in the absence of membranes utilizes an ordered mechanism in which the NDP−sugar donor binds first. (We do not anticipate that the kinetic mechanism will be different on a membrane surface, but this question has yet to be addressed.) Therefore, different members of this superfamily can utilize different kinetic mechanisms.

Different mechanisms with regard to reaction order have also been found to operate with glycosyltransferases belonging to other superfamilies (*27*, *37*−*40*, *55*). Because different mechanisms are possible, it is difficult to predict a priori which substrate to focus on first in the design of crystallization trials to obtain co-complexes with glycosyltransferases. When both the enzyme and the substrates are available in significant quantities, the simplest solution may be to set up numerous crystallizations with both substrates separately and together. When one of the substrates is precious, as it is in our case, it is useful to evaluate the kinetic mechanism. We now know that it is possible in principle to obtain a Michaelis complex with UDP−GlcNAc, and efforts to crystallize *E. coli* MurG with UDP−GlcNAc are underway.

REFERENCES

1. Walsh, C. T. (2000) *Nature 406*, 775−781.
2. Bugg, T. D. H., and Walsh, C. T. (1992) *Natl. Prod. Rep.*, 199−215.
3. Mengin-Lecreulx, D., Texier, L., Rousseau, M., and van Heijenoort, J. (1991) *J. Bacteriol. 173*, 4625−4636.
4. Salmond, G. P. C., Lutkenhaus, J. F., and Donachie, W. D. (1980) *J. Bacteriol. 144*, 438−440.
5. Anderson, J. S., Matsuhashi, M., Haskin, M. A., and Strominger, J. L. (1967) *J. Biol. Chem. 242*, 3180−3190.
6. Men, H., Park, P., Ge, M., and Walker, S. (1998) *J. Am. Chem. Soc. 120*, 2484−2485.
7. Ha, S., Chang, E., Lo, M.-C., Men, H., Park, P., Ge, M., and Walker, S. (1999) *J. Am. Chem. Soc. 121*, 8415−8426.
8. Crouvoisier, M., Mengin-Lecreulx, D., and van Heijenoort, J. (1999) *FEBS Lett. 449*, 289−292.
9. Ikeda, M., Wachi, M., and Matsuhashi, M. (1992) *J. Gen. Appl. Microbiol. 38*, 53−62.

10. Tamura, G., Sasaki, T., Matsuhashi, M., Takatsuki, A., and Yamasaki, M. (1976) *Agric. Biol. Chem. 40*, 447−449.
11. Branstrom, A., Midha, S., Longley, C. B., Han, K., Baizman, E. R., and Axelrod, H. R. (2000) *Anal. Biochem. 280*, 315−319.
12. Bupp, K., and van Heijenoort, J. (1993) *J. Bacteriol. 175*, 1841−1843.
13. Ikeda, M., Wachi, M., Jung, H. K., Ishino, F., and Matsuhashi, M. (1990) *Nucleic Acids Res. 18*, 4014.
14. Mengin-Lecreulx, D., Texier, L., and van Heijenoort, J. (1990) *Nucleic Acids Res. 18*, 2810.
15. Auger, G., Crouvoisier, M., Caroff, M., van Heijenoort, J., and Blanot, D. (1997) *Lett. Pept. Sci. 4*, 371−376.
16. Cudic, P., Behenna, D. C., Yu, M. K., Kruger, R. G., Szewczuk, L. M., and McCafferty, D. G. (2001) *Bioorg. Med. Chem. Lett.*, in press.
17. Ha, S., Walker, D., Shi, Y., and Walker, S. (2000) *Protein Sci. 9*, 1045−1052.
18. Vrielink, A., Ruger, W., Driessen, H. P., and Freemont, P. S. (1994) *EMBO J. 13*, 3413−3422.
19. Morera, S., Lariviere, L., Kurzeck, J., Aschke-Sonnenborn, U., Freemont, P. S., Janin, J., and Ruger, W. (2001) *J. Mol. Biol. 311*, 569−577.
20. A comprehensive and up to date classification of glycosyltransferases: http://afmb.cnrs-mrs.fr/~pedro/CAZY/gtf.html.
21. Mulichak, A. M., Losey, H. C., Walsh, C. T., and Garavito, R. M. (2001) *Structure 9*, 547−557.
22. Ha, S., Gross, B., and Walker, S. (2001) *Curr. Drug Targets: Infect. Disord. 1*, 201−213.
23. Kapitonov, D., and Yu, R. K. (1999) *Glycobiology 9*, 961−978.
24. Ünligil, U. M., and Rini, J. M. (2000) *Curr. Opin. Struct. Biol. 10*, 510−517.
25. Abdian, P. I., Lellouch, A. C., Gautier, C., Ielpi, L., and Geremia, R. A. (2000) *J. Biol. Chem. 275*, 40568−40575.
26. Cleland, W. W. (1963) *Biochim. Biophys. Acta 67*, 104−137.
27. Quiros, L. M., Carbajo, B. J., Brana, A. F., and Salas, J. A. (2000) *J. Biol. Chem. 275*, 11713−11720.
28. Ye, X. Y., Lo, M.-C., Brunner, L., Walker, D., Kahne, D., and Walker, S. (2001) *J. Am. Chem. Soc. 123*, 3155−3156.
29. VanNieuwenhze, M., Mauldin, S., Zia-Ebrahimi, M., Aikins, J. A., and Blaszczak, L. (2001) *J. Am. Chem. Soc. 123*, 6983−6988.
30. Khosla, C., and Harbury, P. B. (2001) *Nature 409*, 247−252.
31. Arita, H., Fukukawa, K., and Matsushima, Y. (1972) *Bull. Chem. Soc. Jpn. 45*, 3611.
32. Sato, K., Miyamoto, O., Inoue, S., Furosawa, F., and Matsuhashi, Y. (1983) *Chem. Lett.*, 725−728.
33. Bannwarth, W., and Tvzeciak, A. (1987) *Helv. Chim. Acta 70*, 175−186.
34. Branch, C. L., Burton, G., and Moss, S. F. (1999) *Synth. Commun. 29*, 2639−2644.
35. Gosselin, S., Alhussaini, M., Streiff, M. B., Takabayashi, K., and Palcic, M. M. (1994) *Anal. Biochem. 220*, 92−97.
36. Purich, D. L. (1996) *Contemporary Enzyme Kinetics and Mechanism*, 2nd ed., Academic Press, New York.
37. Nishikawa, Y., Pegg, W., Paulsen, H., and Schachter, H. (1988) *J. Biol. Chem. 263*, 8270−8281.
38. Ünligil, U. M., Zhou, S., Yuwaraj, S., Sarkar, M., Schachter, H., and Rini, J. M. (2000) *EMBO J. 19*, 5269−5280.
39. Palcic, M. M., Heerze, L. D., Srivastava, O. P., and Hindsgaul, O. (1989) *J. Biol. Chem. 264*, 17174−17181.
40. Qiao, L., Murray, B. W., Shimazaki, M., Schultz, J., and Wong, C.-H. (1996) *J. Am. Chem. Soc. 118*, 7653−7662.
41. Dixon, M. (1979) *Enzymes*, Academic Press, New York.
42. Kamath, V. P., Seto, N. O. L., Compston, C. A., Hindsgaul, O., and Palcic, M. M. (1999) *Glycoconjugate J. 16*, 599−606.
43. Fromm, H. J. (1979) *Methods Enzymol. 63*, 467−486.
44. Bugg, T. D. H., and Brandish, P. E. (1994) *FEMS Microbiol. Lett. 119*, 255−262.
45. Raetz, C. R. H. (1990) *Annu. Rev. Biochem. 59*, 129−170.
46. Feldman, M. F., Marolda, C. L., Monteiro, M. A., Perry, M. B., Parodi, A. J., and Valvano, M. A. (1999) *J. Biol. Chem. 274*, 35129−35138.
47. Imperiali, B., and Zimmerman, J. W. (1990) *Tetrahedron Lett. 31*, 6485−6488.
48. Fang, X., Gibbs, B. S., and Coward, J. K. (1995) *Bioorg. Med. Chem. Lett. 5*, 2701−2706.
49. Rush, J. S., Shelling, J. G., Zingg, N. S., Ray, P. H., and Waechter, C. J. (1993) *J. Biol. Chem. 268*, 13110−13117.
50. Berendes, R., and Jaenicke, L. (1992) *Biol. Chem. 373*, 35−42.
51. Holtje, J.-V. (1998) *Microbiol. Mol. Biol. Rev. 62*, 181−203.
52. Berg, O. G., Gelb, M. H., Tsai, M.-D., and Jain, M. K. (2001) *Chem. Rev. 101*, 2613−2653.
53. Nicholas, R. A., Lamson, D. R., and Schultz, D. E. (1993) *J. Biol. Chem. 268*, 5632−5641.
54. Schwartz, B., Markwalder, J. A., and Wang, Y. (2001) *J. Am. Chem. Soc. 123*, 11638−11643.
55. Kearns, A. E., Campbell, S. C., Westley, J., and Schwartz, N. B. (1991) *Biochemistry 30*, 7477−7483.

BI0256678